INTERSUBBAND PLASMONS IN QUASI-ONE-DIMENSIONAL SYSTEMS

G. Y. HU AND R. F. O'CONNELL
Louisiana State University, Baton Rouge, LA 70803-4001

INTRODUCTION

In a quasi-one-dimensional (Q1D) electronic system, such as a GaAs/AlGaAs quantum wire [1-3], electrons occupy multiple subbands due to the narrow width ($\sim 10^3$Å). Typical values of the energy separation between these subbands are 1 - 3 meV. Intersubband resonance transitions (IRT) between adjacent Q1D subbands have recently been detected and attracted a lot of experimental [1-3] and theoretical attention.[4-6]. In this paper, we give a comprehensive study of the density dependence of the frequency of the IRT plasmon. Also, the coupling between the IRT plasmons is considered. Our new results include a full analysis of the structure of the IRT plasmon between adjacent Q1D subbands and the discovery of a new quantum oscillation phenomenon for the IRT plasmon frequencies (as a function of the electron density).

INTERSUBBAND RESONANCE TRANSITION (IRT) PLASMONS

The physical excitation energies of the Q1D system are determined by the determinant equation[5,6]

$$\det(\varepsilon(q,\omega)) = 0, \tag{1}$$

where $\varepsilon(q,\omega)$ is the dielectric matrix function. Previously [6] we have worked out the form of $\varepsilon(q\to 0,\omega)$ in the RPA approximation and by using the harmonic confinement potential model, where one assumes the electrons are in a xy plane with negligible thickness and a lateral quantized subband energy $\varepsilon_n = (n+\frac{1}{2})\hbar\omega_0$, with n = 0, 1, 2,... and ω_0 the characteristic frequency. According to Ref. 6, at T=0 the relevant matrix elements in (1) for the IRT plasmons between the adjacent levels are (with $|i - j| = 1$):

$$\varepsilon_{ij,ij}(q=0,\omega) = 1 - \frac{2C_i}{\omega+(i-j)\omega_0}, \tag{2a}$$

$$\varepsilon_{ij,ji}(q=0,\omega) = \varepsilon_{ji,ij}(q=0,\omega) = 1 - \frac{2C_i}{\omega+(i-j)\omega_0}, \tag{2b}$$

$$\varepsilon_{ij,lm}(q=0,\omega) = -\frac{1}{[i!j!l!m!]^{1/2}}\frac{2C_i}{\omega+(i-j)\omega_0}, \; l \text{ or } m \neq i,j, \tag{2c}$$

where

$$C_i = \frac{2b^2}{\pi a_B^*}(k_{Fi} - k_{Fj}), \tag{2d}$$

and $b = \sqrt{\hbar/m^*\omega_0}$, $k_{Fi} = \sqrt{2m^*(\varepsilon_F - i\hbar\omega_0)/\hbar^2}$, and $k_{Fi} = 0$ if $\varepsilon_F < i\hbar\omega_0$.

Using (2), after some algebra one deduces from (1) the determinant equation which determines the IRT plasmon for a *M* populated subband system

$$\begin{vmatrix} \gamma^2 - 1 - 2C_0 & -\sqrt{2}C_0 & \cdots & -\dfrac{2C_0}{(M-1)!\sqrt{M}} \\ -\sqrt{2}C_1 & \gamma^2 - 1 - 2C_1 & \cdots & -\dfrac{2C_1}{(M-1)!\sqrt{2M}} \\ \cdots & \cdots & \cdots & \cdots \\ -\dfrac{2C_{M-1}}{(M-1)!\sqrt{M}} & -\dfrac{2C_{M-1}}{(M-1)!\sqrt{2M}} & \cdots & \gamma^2 - 1 - 2C_{M-1} \end{vmatrix} = 0 , \qquad (3)$$

where C_i is defined by (2d). We note that in Ref. 6, we have shown that the IRT plasmon is rigorously decoupled from the intra-subband plasmon as long as the confinement potential is laterally symmetric. Also, we note that the structure of the off-diagonal elements shows that the higher the subband index, the less important is the coupling between the different IRT plasmon modes.

When the coupling between the IRT plasmon modes is neglected (neglecting the off-diagonal elements in (3)), the IRT plasmon frequencies ω_p for a system with M populated subbands can be directly obtained from (3) as

$$\gamma^i \equiv \omega_p^{i+1}/\omega_0 = \left[1 + \frac{4b^2}{\pi a_B^*} (k_{Fi} - k_{Fi+1}) \right]^{1/2} , i = 0,1,\ldots M-1 . \qquad (4)$$

A few comments on (4) are in order. First, there exists M different modes of the intersubband plasmon for a M populated subband system, each representing an electronic collective transition from one subband to its adjacent subband. In addition, one observes $\gamma_0 < \gamma_1 < \ldots < \gamma_{M-1}$, since $k_{Fi} - k_{Fi+1}$ becomes larger for smaller values of i (except for i = M-1, where $k_{FM-1} - k_{FM}$ depends only on the population of the (M -1)th subband). Secondly, it can be shown that among the M different modes, the mode which has the largest value of $(k_{Fi} - k_{F,i+1})$ in (4) has the smallest damping, and is likely the dominant mode being detected by the experiments. Thirdly, from (4) it follows that the dominant mode is either the ω_p^M mode (when the (M-1)th subband is significantly populated) or the ω_p^{M-1} mode (when the (M-1)th subband is almost empty). When the ω_p^M mode dominates we see from (4) and the fact that $k_{FM} = 0$, that the plasmon energy increases with increase of the Fermi energy. When the ω_p^{M-1} mode dominates one can show from (4) that the plasmon energy decreases with the increase of the Fermi energy. Thus, based on the above comments one observes when the magnitude of the gate voltage is increased so to effectively increase ω_0 and decrease ε_F, the plasmon energy displays both an increasing behavior (when the ω_p^{M-1} mode dominates) and a decreasing behavior (when the ω_p^M mode dominates) in consecutive order but the overall trend is an increasing behavior.

The basic feature described above for the intersubband plasmon of an ideal Q1D electron system remains when the mode coupling (the off-diagonal elements) is included by solving (3). When the Q1D system is populated only to the two lowest subbands (M = 0 and 1), there can only be two different IRT plasmon modes. In this case (3) reduces to its top left 2 x 2 matrix, the solution of which can easily be obtained as

$$\gamma_\pm \equiv \omega_p^\pm/\omega_0 = \left[1 + C_0 + C_1 \pm (C_0^2 + C_1^2)^{1/2} \right]^{1/2} . \qquad (5)$$

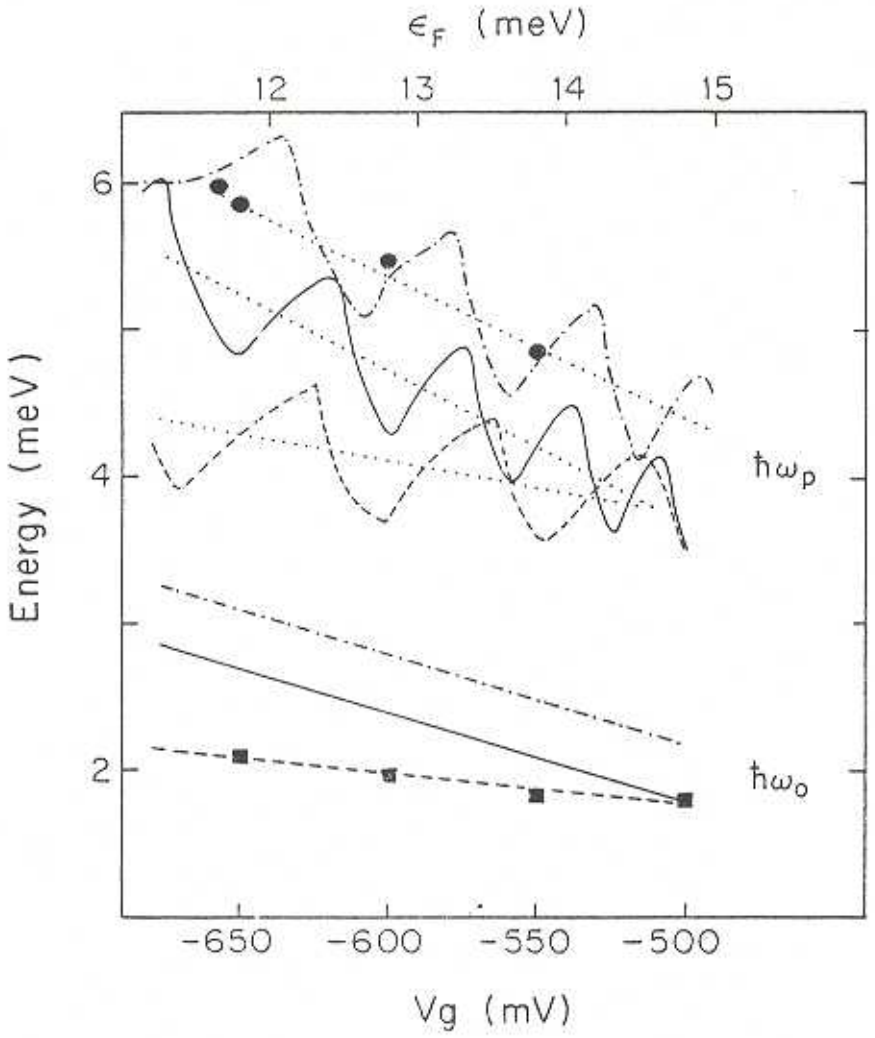

Fig. 1 Intersubband plasmon energy $\hbar\omega_p$ as a function of the gate voltage V_g (the corresponding linear scale of the Fermi energy of the upper axis is chosen by fitting to the experimental data of Ref. 1). Results are presented for three sets of $\hbar\omega_p$ (upper part) calculated at the corresponding different values of the subband separations $\hbar\omega_0$ (lower part). Dotted lines represent values of $\hbar\omega_p$ averaged over its associated periods. Solid squares and circles are the parameters given by Ref. 1, as deduced from the experimental data.

Eq. (5) shows that the coupling of the two modes is not important when $C_1 \to 0$ (the population of the M = 1 subband tends to zero) in which case $\gamma_0 = \gamma_+ = \sqrt{1+2C_0}$ and $\gamma_1 = \gamma_- \approx 1$. They are strongly coupled when C_0 and C_1 are comparable, which pushes the higher frequency mode (here $\gamma_1 = \sqrt{1+2C_1}$) toward the higher coupled mode γ_+ and the lower frequency mode (here $\gamma_0 = \sqrt{1+2C_0}$) toward the lower coupled mode γ_-. For example, it is straightforward to obtain $\gamma_+ = \sqrt{1+3C_1}$ from (5) when $\varepsilon_F = 2\hbar\omega_0$.

This coupled IRT plasmon modes picture can directly be extended to a Q1D system with M populated subbands, where the original M IRT plasmon modes are coupled into M new modes possessing different frequencies than the uncoupled ones. On the other hand, as the mode involved with higher subband index i has smaller coupling (see the off-diagonal elements in Eq. (3)), the IRT plasmons in the many subbands system is not just a simple extended picture of the M = 2 case. In other words, to obtain an accurate analysis of the multiple IRT plasmons, one should solve (3) exactly. In Fig. 1, we present our numerical solution of (3) for the dominant mode of the IRT plasmons, where the values of M (5 - 10) and ω_0(1 - 3 meV) are chosen in the range comparable to that of the experiments. The figure shows that when one increases the magnitude of the gate voltage so to effectively increase ω_0 and decrease ε_F the IRT plasmon energy displays both an increasing behavior (when the ω_p^{M-1} mode dominates) and a decreasing behavior (when the ω_p^M mode dominates) in consecutive order but the overall trend is an increasing behavior.

The actual value of the ω_0 and the electron density may be slightly different for each individual wire in the sample. Therefore, we propose that the actual measured $\hbar\omega_p$ in the experiments of Hansen et al. (whose 1D multiwire structures contained $\approx 10^4$ wires) corresponds to the averaged value of $\hbar\omega_p$ (dotted line) shown in that figure. On the other hand, our results do imply that the quantum oscillation behavior discussed here should be observable for an ideal sample.

The work was supported in part by the U. S. Office of Naval Research under grant No. N00014-90-J-1124.

REFERENCES

1. W. Hansen, M. Horst, J. P. Kotthaus, U. Merkt, Ch. Sikorski, and K. Ploog, Phys. Rev. Lett. **58**, 2586 (1987); F. Brinkop, W. Hansen, J. P. Kotthaus, and K. Ploog, Phys. Rev. B **37**, 6547 (1988).
2. T. Demel, D. Heitmann, P. Grambow, and K. Ploog, Phys. Rev. **B38**, 12732 (1988).
3. T. P. Smith III, J. A. Brum, J. M. Hong, C. M. Knoedler, H. Arnot, and L. Esaki, Phys. Rev. Lett. **61**, 585 (1988).
4. W. Que and G. Kirczenow, Phys. Rev. **37**, 7153 (1988).
5. Qiang Li and S. Das Sarma, Phys. Rev. **B40**, 5860 (1989).
6. G. Y. Hu and R. F. O'Connell, Phys. Rev. B **42**, 1290 (1990).
7. G. Y. Hu and R. F. O'Connell, J. Phys. C, to appear.